Available online at www.sciencedirect.com
SCIENCE DIRECT®
European Journal of Pharmaceutics and Biopharmaceutics 63 (2006) 156–165
European Journal of Pharmaceutics and Biopharmaceutics
www.elsevier.com/locate/ejpb

Research paper

Fluorescence resonance energy transfer: Evaluation of the intracellular stability of polyplexes

Miriam Breunig, Uta Lungwitz, Renate Liebl, Achim Goepferich *

Department of Pharmaceutical Technology, University of Regensburg, Regensburg, Germany

Received 18 November 2005; accepted in revised form 27 January 2006
Available online 9 March 2006

Abstract

The investigation of intracellular mechanisms of non-viral nucleic acid delivery systems has provided great impetus for the improvement of their efficacy. Especially the intracellular release of the nucleic acid from the non-viral carrier system may be a relevant criterion for the high transfection efficiency of certain polymers. Therefore, we evaluated fluorescence resonance energy transfer (FRET) in combination with confocal laser scanning microscopy or flow cytometry as tool to determine the intracellular disintegration of polyplexes built with plasmid DNA and linear polyethylenimine. In microscopy, which allowed for an observation of polyplexes within single cells, sensitized emission measurement and acceptor photobleaching have been tested towards quantitative FRET analysis. In contrast, the whole cell population was analyzed by the flow cytometry-based method. We suggest that FRET is a useful tool to evaluate the intracellular disintegration of polyplexes built with various polymers.

Keywords: Non-viral gene delivery; Polyethylenimine; Fluorescence resonance energy transfer; Confocal laser scanning microscopy; Flow cytometry

1. Introduction

In order for non-viral nucleic acid delivery systems to become a real alternative to viral vectors, the transfection efficiency must be substantially increased. Due to its relatively high efficiency, polyethylenimine (PEI), available in both branched (BPEI) and linear (LPEI) forms, has gained some prominence compared to other non-viral gene delivery systems. PEI is capable of condensing DNA into polyplexes, allowing for the cellular uptake of DNA. Once the polyplexes enter the endo-lysosomal compartment, PEI guides the minimally degraded DNA into the cytoplasm and finally to the nucleus to be transcribed [1–4]. To further optimize the transfection efficiency of PEI-based delivery systems, it would be useful to investigate the interactions of polyplexes with cells and the intracellular mechanisms involved in the transfection process.

Some of the unique properties of PEI include its efficient condensation and protection of DNA extracellularly and its capability to release the DNA, even if only partially, intracellularly. For the investigation of the interaction of plasmid DNA and polymer, both components of polyplexes have been labeled with fluorescent dyes and observed by confocal laser scanning microscopy (CLSM) [5,6]. However, investigations are often hampered by the limited spatial resolution of conventional widefield fluorescence microscopy. The application of a fluorescence resonance energy transfer (FRET)-based technique would allow for more precise distance measurements in the range of 1–10 nm.

So far, only two studies have utilized a FRET-based approach for the determination of the complexation state of intracellular polyplexes: Itaka et al. [7] made observations concerning the condensation of double labeled plasmid DNA in intracellular polyplexes. The conformational change of plasmid DNA after condensation with polymer, which would lead to a change in the distance between two

* Corresponding author. Department of Pharmaceutical Technology, University of Regensburg, Universitaetsstrasse 31, 93040 Regensburg, Germany. Tel.: +49 0 941 943 4843; fax: +49 0 941 943 4807.
E-mail address: achim.goepferich@chemie.uni-regensburg.de (A. Goepferich).

0939-6411/$ - see front matter © 2006 Elsevier B.V. All rights reserved.
doi:10.1016/j.ejpb.2006.01.012

fluorescent molecules attached to plasmid DNA, was detected. For analyzing FRET the fluorescence intensity ratio of the fluorescent dyes was calculated at each pixel and an image in gray scale was created to express the ratios. A decrease in the FRET efficiency of plasmid DNA in LPEI-polyplexes due to disintegration was observed after intracellular uptake, while plasmid DNA retained high FRET efficiency in BPEI-polyplexes indicating that the DNA was kept in a condensed state. However, the selection of the filter set in this measurement enables a cross-talk of the selected dyes that is not considered during the calculation of the ratio images. Nevertheless, the method can be applied in the described case, because the molar ratio of the two fluorescent dyes is constant. Similarly, Kong et al. [8] observed the decondensation of BPEI-polyplexes within cells, when plasmid DNA and BPEI were separately labeled with Alexa Fluor 488 and rhodamine, respectively. The degree of energy transfer within the polyplexes was evaluated by the ratio between the average intensity of Alexa Fluor 488 and rhodamine emission at a given location. Unfortunately, a possible cross-talk and varying concentrations of fluorescent dyes in polyplexes were not considered. In conclusion, while both experimental designs are interesting, neither approach supplied the determination of a FRET efficiency.

Therefore, we evaluated whether various methods for the investigation of FRET described in the literature are applicable to determine the stability of intracellular LPEI-polyplexes. To this end, each component of the polyplexes, i.e., polymer and plasmid DNA, was labeled with a fluorescent dye and FRET was measured using both microscopy and flow cytometry.

2. Theory of FRET and measuring techniques

FRET is a process by which a fluorophore (the donor) in an excited state transfers its energy to a neighboring molecule (the acceptor) by non-radiative dipole–dipole interaction [9–12]. One of the most important factors influencing the efficiency of energy transfer is the distance between the donor and acceptor dye molecules (Fig. 1). Energy transfer within the 1–10 nm distance range correlates well with the macromolecular dimension [13] and is, therefore, capable of resolving distances much shorter than the inherent diffraction limit of conventional microscopy. When FRET occurs, there is a net gain in the energy of emission by the acceptor at the expense of the fluorescence emitted from the donor (donor quenching); this process is called sensitized emission (Fig. 2).

For FRET to occur efficiently:

1. The donor must have a high quantum yield.
2. The emission spectrum of the donor must overlap with the absorption spectrum of the acceptor (Fig. 2).
3. The donor and acceptor molecules must be in close proximity (typically 1–10 nm).
4. The absorption and emission moments and their separation vector must be appropriately aligned.

According to the theory of Förster the transfer efficiency (E) is defined as the probability of decay of the excited donor molecules due to energy transfer as compared to the total number of decay events, and is given by (for reviews, see [14,15])

$$E = \frac{k_T}{k_T + k_F + k_D}, \quad (1)$$

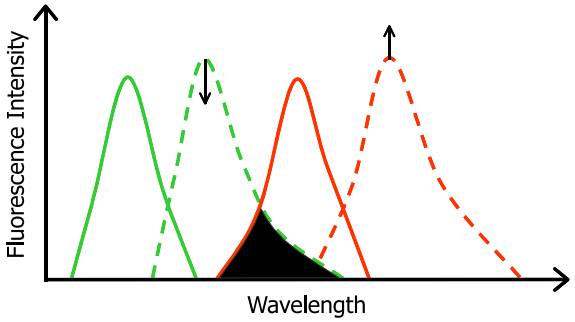

Fig. 2. Fluorescence excitation and emission spectra of a FRET donor–acceptor pair. The spectra from left to right represent: donor excitation (solid line), donor emission (dashed line), acceptor excitation (solid line), and acceptor emission (dashed line). Sensitized emission requires the excitation of the donor and then the detection of the acceptor emission. Upon FRET the donor emission decreases (↓), while the acceptor emission increases (↑). The gray region indicates the overlap of the donor emission spectrum and the absorption spectrum of the acceptor.

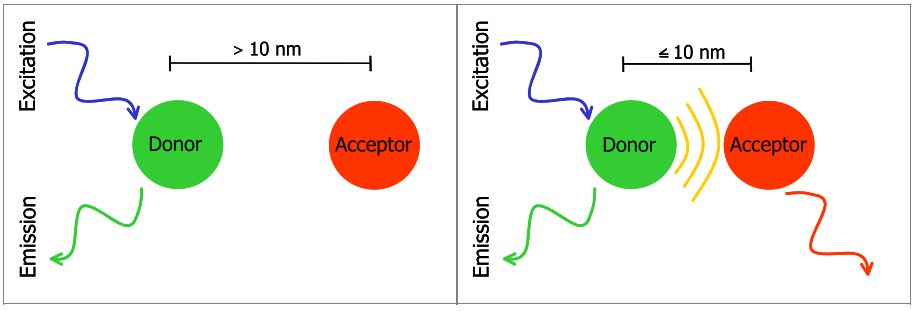

Fig. 1. FRET is the non-radiative transfer of photon energy from an excited fluorophore (the donor) to another fluorophore (the acceptor) when both are located within close proximity (1–10 nm) (adapted from [20]).

where k_T is of the rate constant of the transfer process, k_F is the rate constant of fluorescence emission of the donor, and k_D is the sum of the rate constants of all other de-excitation processes of the donor.

The rate of energy transfer (k_T) can also be expressed by

$$k_T = \text{const } k_F J n^{-4} R^{-6} \kappa^2, \tag{2}$$

where R is the distance between the donor and acceptor molecules, and κ^2 is an orientation factor describing the relative orientation of the donor's emission dipole and the acceptor's absorption dipole in space. The overlap integral J represents the degree of overlap between the donor fluorescence spectrum and the donor absorption spectrum, and n is the refractive index of the medium.

Furthermore, E depends on the inverse sixth power of the distance between the donor and the acceptor, and hence quickly decreases with an increase of R

$$E = \frac{R^{-6}}{R^{-6} + R_0^{-6}}, \tag{3}$$

where R_0 is the characteristic separation distance of each dye pair, defined as the distance at which the probability of energy transfer is 50%. From Eqs. (1)–(3) the rate k_T of energy transfer is also defined by

$$k_T = \frac{1}{\tau}\left(\frac{R_0}{R}\right)^6, \tag{4}$$

where τ is the donor lifetime in the absence of the acceptor. As the fluorescence lifetime of a fluorophore is the characteristic time that a molecule exists in the excited state prior to returning to the ground state, time-resolved FRET measurements can be used to perform experiments with greater accuracy.

For distance measurements to be quantitative, FRET methods have to account for 'bleed-through' in excitation, when the donor is excited by the excitation wavelength of the acceptor, and 'cross-talk' in emission detection, when the emission of a donor also contributes to the signal measured in a setup for acceptor detection, and vice versa.

FRET associated with cells can be measured by different means, the two most common methods being microscopy and flow cytometry. While a whole cell population can be analyzed by flow cytometry, the distribution of FRET events within a single cell can be elucidated using fluorescence microscopy. In microscopy, two main approaches have been established towards quantitative FRET analysis: sensitized emission measurement and acceptor photobleaching.

2.1. Sensitized emission in microscopy

Sensitized emission is the most common approach towards quantitative FRET. It requires the excitation of the donor and the detection of light emitted by either the donor and/or the acceptor in the presence of the other fluorophore. When FRET occurs, the intensity of donor emission is decreased and that of the acceptor emission is increased. Various methods have been applied to measure FRET from changes in donor and acceptor emission [16–19]. In the following, three different methods for the quantitative determination of sensitized emission in CLSM reported in the literature are described [17–19] (the calculations may be performed with a software tool from Carl Zeiss Co. Ltd., Germany [20]). For each measurement at least three samples are required; the donor (d) and acceptor (a) controls and the experimental sample (f). Furthermore, a combination of three filter sets for the detection of the donor fluorescence (D), the acceptor fluorescence due to direct excitation (A) or due to FRET (F) is used for the measurement of each sample.

According to [20] the calculation of three different FRET values for sensitized emission is possible, (i) *Fc* (FRET corrected), (ii) *Fn* (FRET net), and (iii) *NF* (normalized FRET). In the following equations [20], the uppercase letter denotes the filter set and the lowercase letter indicates which fluorophores are present in the specimen (as described above in brackets), for example *Fd* indicates that the donor is labeled (d) and the donor fluorophore is excited and the emission is detected in the acceptor channel (F).

(i) The method according to Youvan et al. [19] (calculation of *Fc*) simply determines a FRET intensity image corrected by the cross-talk and background intensity, but is not normalized for the concentration of the donor and acceptor. This means that the FRET values are proportional to the donor and acceptor concentration and that high *Fc* numbers occur when high concentration of donor and acceptor is present

$$Fc = Ff - \left[\frac{Fd}{Dd} \cdot Df\right] - \left[\frac{Fa}{Aa} \cdot Af\right]. \tag{5}$$

Fd/*Dd* is a measure for the ratio of the donor signal detected in the FRET channel and in the donor channel, while *Fa*/*Aa* is a measure for the ratio of the acceptor signal detected in the FRET channel and in the acceptor channel. The terms *Df* and *Af* correlate with the donor and acceptor concentration, respectively. Thus, the FRET value *Ff* can be corrected by the direct contribution of the donor and acceptor, their cross-talk and concentration, namely *Donor corr* and *Acceptor corr*, to get *Fc* according to Youvan et al.

$$Fc = Ff - [\text{Donor corr}] - [\text{Acceptor corr}]. \tag{6}$$

(ii) According to Gordon et al. [17] (*Fn*) the image resulting from calculation of *Fc* should be additionally normalized to the donor and acceptor signals. This method may be of special interest when structures with low intensities are investigated. However, it also overcompensates for concentration, resulting in FRET values that are inversely proportional to the concentration

$$Fn = \frac{Ff - [\text{Donor corr}] - [\text{Acceptor corr}]}{G \cdot Fd \cdot Fa}. \tag{7}$$

The parameter G relates the sensitized emission to the decrease of donor fluorescence attributable to FRET.

(iii) In the analysis described by Xia and Liu [18] (NF), the corrected FRET image is divided by the square root of the product of donor and acceptor. Hence, the FRET efficiency should be constant and independent of the local concentration of donor and acceptor.

$$NF = \frac{Ff - [\text{Donor corr}] - [\text{Acceptor corr}]}{\sqrt{G \cdot Fd \cdot Fa}}. \quad (8)$$

2.2. Acceptor photobleaching in microscopy

Another approach to detect FRET by microscopy is acceptor photobleaching [16,21–25]. The donor is excited and its emission is detected before and after acceptor photobleaching. After the acceptor is bleached or chemically destroyed, the donor signal increases since no energy transfer to the acceptor is possible. Such an increase in fluorescence following bleaching is characteristic for FRET, because fluorescence normally decreases following a bleach. An advantage of acceptor photobleaching is that corrections are not necessary because an increase in donor fluorescence cannot be related to acceptor bleed-through.

For the measurement, a FRET positive and negative control and the spectral references are required. In a time series with about 2–5 pre-bleach images, the acceptor should be bleached to about 20% and imaging should continue after bleaching. The FRET efficiency E is calculated from photobleaching kinetics of the donor in the presence and absence of the acceptor in pixels or regions of interest (ROIs) using the following equation [25]:

$$E = \frac{F_{\text{Donor max}} - F_{\text{Donor min}}}{F_{\text{Donor max}}}. \quad (9)$$

Linear regression of the fluorescence intensity of the donor F_{Donor} versus acceptor F_{Acceptor} allows for the determination of $F_{\text{Donor max}}$, while $F_{\text{Donor min}}$ is obtained as average value of the fluorescence intensity of the donor from a time series of about 2–10 pre-bleach images.

2.3. FRET measurements in flow cytometry

Flow cytometry enables the statistical analysis of the distribution of FRET events in a cell population. In addition to the controls needed for microscopy, an additional sample of unlabeled cells is required to account for the cell autofluorescence [15,26,27].

In the following equations it is assumed that the donor fluorescence is excited with a 488 nm laser line and detected at 530 nm [$I_1(488 \rightarrow 530)$] and a laser emitting light of 635 nm is used to excite the acceptor which is recorded at 661 nm [$I_3(635 \rightarrow 661)$]. Sensitized acceptor emission is detected with excitation at 488 nm and emission at >670 nm [$I_2(488 \rightarrow >670)$].

The simplest approach to measure energy transfer would be to determine the decrease in the fluorescence of the donor in the presence of the acceptor. Donor quenching (ET) can be calculated from mean fluorescence intensity of flow cytometry measurements according to [28]

$$ET = \frac{F_{1,0}(488,530) - F_{1,1}(488,530)}{F_{1,0}(488,530)}, \quad (10)$$

where $F_{d,\,a}(x,y)$ represents the mean fluorescence intensity obtained in the absence ($d = 0$) or presence ($d = 1$) of a donor, in the absence ($a = 0$) or presence ($a = 1$) of an acceptor after excitation at x nm and detection at y nm.

The acceptor sensitized emission is expressed by the energy transfer parameter (ET_{p}) [28]

$$ET_p = \frac{F_{1,1}(488,670) - (F_{1,1}(488,530)/a) - (F_{1,1}(635,670)/b)}{F_{1,1}(488,670)}. \quad (11)$$

The factors a and b are used to correct by the direct contribution of donor and acceptor in samples with donor or acceptor labeled only, respectively:

$$a = \frac{F_{1,0}(488,530)}{F_{1,0}(488,670)} \quad (12)$$

and

$$b = \frac{F_{0,1}(635,670)}{F_{0,1}(488,670)}. \quad (13)$$

These calculations provide a single mean FRET value for the whole cell population. However, sensitized emission can also be applied to calculate the distribution of the transfer efficiency on a cell-by-cell basis. Szollossi and coworkers reported the technical details and computer-based methods for calculation of the FRET efficiency in various papers [15,26,29–31].

Briefly, a correction factor α, which represents the correction due to the different detectability of the donor and acceptor fluorescence, is determined by the following formula:

$$\alpha = \frac{F_{0,1}(488,670) \cdot r_{\text{Donor}} \cdot \varepsilon_{\text{Donor, 488}}}{F_{1,0}(488,530) \cdot r_{\text{Acceptor}} \cdot \varepsilon_{\text{Acceptor, 488}}}. \quad (14)$$

The numerical value of α is determined from the fluorescence intensities of cells saturated with either donor or acceptor label. Furthermore, the molar extinction coefficients ε and the conjungate-to-dye ratio r are required. The sensitized emission has to be corrected for the direct contribution of the donor. The S_1 correction factor is determined from cells labeled with donor only and calculated using the following formula:

$$S_1 = \frac{F_{1,0}(488,670)}{F_{1,0}(488,530)} = \frac{I_2}{I_1}. \quad (15)$$

The sensitized emission has also to be corrected by the contribution of the acceptor which may suboptimally be excited at 488 nm. The correction factor S_2 is determined from cells with acceptor labeled only:

$$S_2 = \frac{F_{0,1}(488,670)}{F_{0,1}(635,670)} = \frac{I_2}{I_3}. \quad (16)$$

Furthermore, the acceptor emission is corrected for the direct contribution of the donor which may suboptimally be excited by 635 nm. The S_3 correction factor is determined from cells labeled with donor only and is calculated as follows:

$$S_3 = \frac{F_{1,0}(635,670)}{F_{1,0}(488,530)} = \frac{I_3}{I_1}. \quad (17)$$

Furthermore, the three recorded fluorescence intensities I_1, I_2, and I_3 can be expressed as follows:

$$I_1(488 \rightarrow 530) = I_D(1-E), \quad (18)$$

$$I_2(488 \rightarrow > 670) = I_D(1-E)S_1 + I_A S_2 + I_D E\alpha, \quad (19)$$

$$I_3(635 \rightarrow 661) = I_D(1-E)S_3 + I_A + S_3/S_1 I_D E\alpha. \quad (20)$$

I_D and I_A express the non-quenched and non-enhanced intensities of the donor and acceptor, respectively. Calculating these equations, an intermediate value A is obtained:

$$A = \frac{E}{1-E} = \frac{1}{\alpha}\left[\frac{(I_2 - S_2 I_3)}{\left(1 - \frac{S_3 S_2}{S_1}\right) I_1} - S_1\right]. \quad (21)$$

Finally, the FRET efficiency E can be calculated by the following formula:

$$E = \frac{A}{1+A}. \quad (22)$$

3. Materials and methods

3.1. Plasmid DNA labeling

When indicated, plasmid DNA (pEGFP-N1, Clontech) was either covalently labeled with Alexa Fluor 488 according to the manufacturer's protocol (ULYSIS Nucleic acid labeling kit, Molecular Probes, The Netherlands) or stained with the intercalating dye YOYO-1 (Molecular Probes, The Netherlands). The labeling reaction with YOYO-1 was carried out with a molar ratio of 1 dye molecule per 320 base pairs at room temperature in the dark.

Non-covalent staining of plasmid DNA is possible, because YOYO-1 has a high affinity for nucleic acids [32]. Indeed, the intercalating dye may be displaced during condensation with the polycation [33] or the fluorescence quantum yield may be decreased [34], however appropriate control samples were applied which show the same effect. Furthermore, FRET experiments with intercalating dyes have successfully been applied so far [35,36]. In contrast, to avoid diffusion of the fluorophore during the time frame of photobleach experiments (five minutes and longer), the plasmid DNA was covalently labeled with Alexa Fluor 488. It should be mentioned that both labeling methods may change the structure, behavior, and stability of polyplexes compared to unlabeled ones, hence, the ratio of dye to base pairs was kept as low as possible and controls were mandatory.

3.2. Non-viral carriers

LPEI with a M_W of 5.0 kDa was synthesized as previously described [37]. When indicated, the polymer was labeled with 6-TAMRA-succinimidyl ester or Alexa Fluor 633 (both Molecular Probes, The Netherlands) as described [6]. In the following, the notation of LPEI was made without the unit kDa.

3.3. Preparation of polyplexes

Plasmid DNA/LPEI complexes were prepared at NP ratios (ratio of nitrogens in polymer to phosphates in DNA) of 6, 18 or 30 in 150 mM sodium chloride as described [6]. In the following, the notation of polyplexes was made without the unit kDa; LPEI 5.0 – polyplexes indicates that polyplexes were built with LPEI 5.0.

3.4. CLSM experiments

A Zeiss Axiovert 200 M microscope coupled to a Zeiss LSM 510 scanning device (Carl Zeiss Co. Ltd., Germany) was used for CLSM experiments. The inverted microscope was equipped with a Plan-Apochromat 63× objective. CHO-K1 cells were plated in 8-well Lab-Tek™ Chambered Coverglass (Nunc GmbH & Co. KG, Germany) at an initial density of 35,000 cells/chamber in a volume of 400 μl culture medium (Ham's F12, Sigma–Aldrich GmbH, Germany). 20 mM HEPES (Ham's F12, Sigma–Aldrich GmbH, Germany) was added to the medium to maintain a pH of 7.4. After 18 h, polyplexes were added and measurements were directly performed in each well at 37 °C. The thickness of the optical sections was between 0.7 and 1.2 μm.

3.4.1. Sensitized emission

FRET values for sensitized emission were calculated with the FRET Macro software tool from Carl Zeiss Co. Ltd. (Germany) [20]. The specimens used to acquire the raw data were: CHO-K1 cells incubated with polyplexes at NP 6 with donor labeled only (DNA in polyplexes labeled with YOYO-1), acceptor labeled only (LPEI 5.0 in polyplexes labeled with TAMRA), and the FRET specimen (double labeled polyplexes). The donor YOYO-1 was excited with a 488 nm argon laser and detected with a 505–530 nm bandpass filter, while TAMRA was detected with a 560–615 nm bandpass filter after excitation with 543 nm. Each specimen was acquired in a multitrack configuration with three tracks: donor excitation/donor emission detection (D: donor track), acceptor excitation/acceptor emission detection (A: acceptor track), and donor excitation/acceptor emission detection (F: FRET track). For the determination of the location of polyplexes a transmitted light image was also recorded.

3.4.2. Acceptor photobleaching

The acceptor photobleaching method was applied for polyplexes at NP 6 consisting of TAMRA-labeled LPEI

5.0 and Alexa Fluor 488-labeled DNA incubated with CHO-K1 cells. As controls, polyplexes with only the donor labeled were used. Images were taken in the multitracking modus with the configuration of filters for the donor and acceptor tracks without the FRET track as described above. Bleaching was conducted by scanning a region of interest 12 times using the 543 nm argon laser line at 100% intensity. Each time the whole cells were bleached to avoid unwanted fluorescence recovery after photobleaching (FRAP) effects. Before and after this bleach, Alexa Fluor 488 and TAMRA images were recorded to assess changes in donor and acceptor fluorescence. Any increase in Alexa Fluor 488 fluorescence caused by bleaching of the TAMRA acceptor could be concealed by bleaching of Alexa Fluor 488 related to the imaging process itself. Hence, to ensure that bleaching due to imaging was minimal, the level of bleaching in each experiment was monitored by collecting Alexa Fluor 488/TAMRA image pairs before and after the bleach.

3.4.3. Flow cytometry

CHO-K1 cells were grown in 24-well plates at an initial density of 38,000 cells per well. Eighteen hours after plating, the prepared polyplexes were added to the cells. After 6 h of transfection with polyplexes with donor labeled only (DNA in polyplexes labeled with YOYO-1), acceptor labeled only (LPEI 5.0 in polyplexes labeled with Alexa Fluor 633), and double labeled polyplexes, cells were prepared for flow cytometry analysis as described previously [6]. Untreated cells were used to determine the autofluorescence of cells. As the value for donor quenching is sensitive to the concentration of the fluorophores, the concentration of donor and acceptor should be saturated. However, the concentration of fluorophores in polyplexes with various NP ratios may most likely never be saturated. Therefore, to take account of the varying concentration and to minimize the error in calculations, a separate set of acceptor only labeled sample was used to calculate the donor quenching at each NP ratio. Measurements were taken on a FACSCalibur (Becton–Dickinson, Germany) using CellQuest Pro software (Becton–Dickinson, Germany) and WinMDI 2.8 (©1993–2000 Joseph Trotter). YOYO-1 was excited using a 488 nm argon laser and detected with a 530 ± 30 nm bandpass filter, while Alexa Fluor 633 was excited with 635 nm and detected with a 661 ± 8 nm bandpass filter. Sensitized acceptor emission was detected with excitation at 488 nm and emission at >670 nm.

4. Results and discussion

Previous observations of double labeled LPEI 5.0-polyplexes by CLSM indicated that polyplexes remained intact extracellularly, but once entered the cell at least a part dissociated or seemed to form loose aggregates [6]. However, the evaluation of interaction of LPEI and plasmid DNA in confocal images is very time consuming and may be limited by the spatial resolution in microscopy. Therefore, FRET was introduced as tool to investigate the interaction of plasmid DNA and LPEI in polyplexes.

4.1. Sensitized emission in microscopy

For measurement of the sensitized emission of double labeled LPEI 5.0-polyplexes at NP 6 in CHO-K1 cells, three samples, the donor and acceptor control and the FRET sample, were analyzed. To evaluate the location of polyplexes within the cells, the calculated FRET ratio images were directly compared to an image showing both the donor and acceptor channels as well as the transmitted light channel (Fig. 3A). In this image, extracellular polyplexes were characterized by an overlay of green and red, respectively, plasmid DNA and LPEI, indicating a close interaction between polymer and plasmid DNA. Some of the intracellular polyplexes seemed to disintegrate. Figs. 3B–D show the corresponding calculated FRET ratio images according to Youvan (Fig. 3B), Gordon (Fig. 3C), and Xia (Fig. 3D). The colored pixels indicate a FRET efficiency from 0 (dark blue) to 100% (white). For a direct comparison with Fig. 3A, the ratio image D according to Xia et al. was chosen because it is independent of the concentration of the fluorescent dyes, which is most appropriate for LPEI-polyplexes. Fig. 3B does not take the concentration of the two fluorophores into account and Fig. 3C overcompensates for the concentration.

Comparing Figs. 3A and D, extracellular polyplex aggregates were represented by colored pixels with FRET efficiencies of about 30–90%. The values for the FRET efficiency varied within polyplexes, indicating that the extent of interaction between polymer and plasmid DNA in extracellular polyplexes was not equally distributed. Furthermore, it was less time consuming to detect FRET events in intracellular polyplexes in the ratio images compared to Fig. 3A because it was not necessary to zoom into the images for a careful evaluation of each polyplex. Intracellular polyplexes that seemed to disintegrate in Fig. 3A consisted of green, red, and yellow areas, representing plasmid DNA, polymer, and an overlay of both. In times when an overlay of red and green was detected in Fig. 3A, a corresponding FRET efficiency ranging from 40% to 90% was also visible in Fig. 3D, but not in areas where only a green or red fluorescence was detected. Thus, the FRET results were reasonable and indicated that intracellular polyplexes disintegrated, but the contact between polymer and DNA was still very close in certain areas.

4.2. Acceptor photobleaching in microscopy

Double labeled LPEI 5.0-polyplexes at NP 6 were used to evaluate the acceptor photobleach method. According to this procedure, if FRET occurs, photobleaching of the acceptor (TAMRA) should yield a significant increase in the fluorescence of the donor (Alexa Fluor 488). To mini-

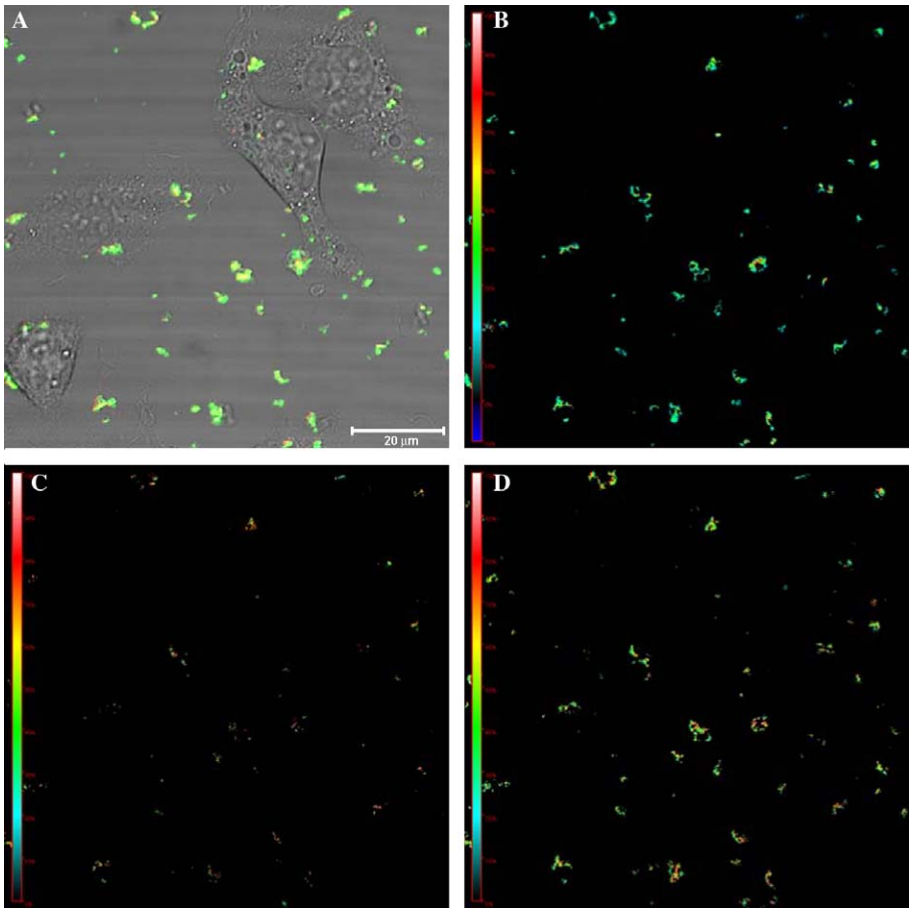

Fig. 3. Sensitized emission measurements of LPEI 5.0-polyplexes at NP 6 in CHO-K1 cells by CLSM. (A) Observing double labeled LPEI-polyplexes in the multitracking mode, DNA is represented by green dots and polymer by red dots. A colocalization of both would yield a mixture color of yellow. To evaluate the location of polyplexes with regard to the cells, a transmitted light image was also recorded. The bar indicates 20 µm. (B–D) Corresponding calculated FRET ratio images according to Youvan (B), Gordon (C), and Xia (D). The colored pixels were calculated according to [20] and indicate a FRET efficiency from 0 (dark blue) to 100% (white) as indicated by the sidebars.

mize the effect of photobleaching due to imaging, images of Alexa Fluor 488 were collected at low laser intensity. The intensity of a certain number of Alexa Fluor 488-labeled polyplexes remained nearly constant during a time series of 15 images, but sometimes also varied (about 5%) during imaging, most likely due to polyplex movements during imaging (data not shown). As a negative control, acceptor photobleaching of cells transfected with polyplexes stained with Alexa Fluor 488 alone was conducted, while larger extracellular polyplex aggregates and smaller intracellular polyplexes were evaluated. In these samples, FRET should be impossible, because the acceptor fluorophore TAMRA is absent. The fluorescence intensity decreased during imaging and bleaching, especially in smaller polyplexes (Fig. 4A, lower curve). This decrease in fluorescence intensity could be due to an unwanted bleaching of the donor or, as discussed above, due to movements of the polyplexes, the cells or even stage drift during the imaging process. However, immediately after bleaching, the fluorescence intensity of larger polyplexes (Fig. 4A, upper curve) and smaller polyplexes (Fig. 4A, lower curve) seemed to remain constant.

As the simplest approach to evaluate whether our acceptor photobleaching protocol was feasible, the FRET efficiencies from 10 bleached extracellular polyplexes were measured and calculated as positive control. Fig. 4B shows an example of such a polyplex, after bleaching the acceptor (lower curve) the fluorescence of the donor (upper curve) substantially increased, the calculated FRET efficiency was 62.03%. This effect was reproducible for a set of 10 different polyplexes. The acceptor fluorophor TAMRA was not very effectively bleached by the applied method, but additional bleaching iterations led to a decrease in the intensity of Alexa Fluor 488 in the negative control. To test the intracellular polyplexes, the whole cell was bleached to avoid FRAP effects, but the intensity was calculated from a defined region containing intracellular green and red spots, respectively, polyplexes. In the example shown in Fig. 5, the FRET efficiency of an area containing about eight intracellular polyplexes that seemed to dissociate was calculated, it had a value of 30.5%. This pattern was reproducible for intracellular polyplexes of about 10 cells. The FRET efficiencies were not as high as for the positive control, indicating the interaction between polymer and

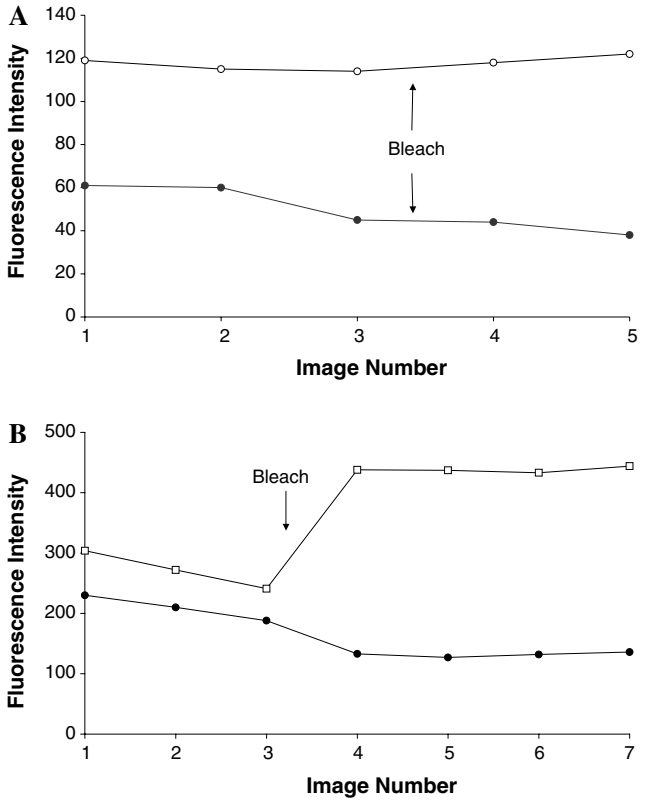

Fig. 4. Acceptor photobleaching of LPEI 5.0-polyplexes at NP 6 in CHO-K1 cells. (A) As negative control cells transfected with polyplexes that were labeled with Alexa Fluor 488 alone were used. The fluorescence intensity of larger polyplexes (upper curve) and smaller polyplexes (lower curve) was quantified by averaging the fluorescence within one ROI of a certain number of polyplexes. Some bleaching due to imaging occurred at all time points except the one immediately after the bleach where constancy was detected. (B) As positive control extracellular double labeled polyplexes were used. After bleaching the acceptor TAMRA (lower curve) the fluorescence of the donor Alexa Fluor 488 (upper curve) substantially increased.

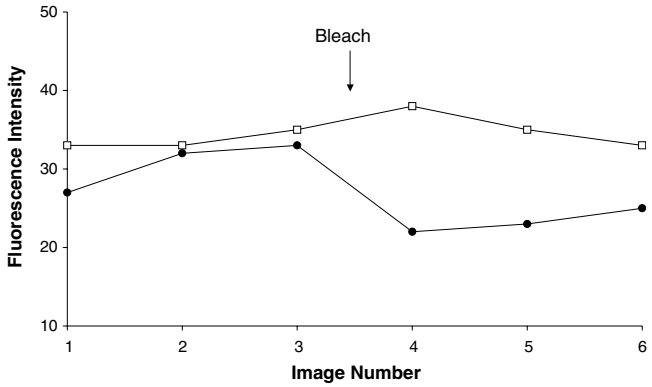

Fig. 5. Acceptor photobleach of eight intracellular double labeled LPEI 5.0-polyplexes that appeared to dissociate as shown by the fluorescence intensity of Alexa Fluor 488 (upper curve) and TAMRA (lower curve) during imaging. After bleaching the acceptor the fluorescence of the donor slightly increased.

plasmid DNA was not as close as in extracellular polyplexes. However, the results were not accurate because some polyplexes, especially the smaller ones, disappeared due to drift of the stage or polyplex and cell movements (in and out of the z-stack) during the imaging and bleaching process. The acceptor photobleaching can only be applied given the fact that the time between pre- and post-bleaching is not too long to allow for movements of or in the sample. In the samples shown, the pre- and post-bleach images and the bleaching itself took about 5 min and sample movement was visible in sequentially recorded images (data not shown). Additionally, image sets recorded with frame-wise multitracking may show a delay between the same pixel position for different channels. These problems are more pronounced in living cells compared to fixed samples. However, in our opinion, fixed samples do not reflect the situation as well as living samples, because the fixing agents alter the structure of polyplexes (data not shown). The choice of fluorescent dyes that are more readily bleached than TAMRA may help to solve the problem, but only in part.

4.3. Flow cytometry

For the evaluation of interaction between polymer and plasmid DNA in intracellular polyplexes, donor quenching of double labeled LPEI 5.0-polyplexes (with YOYO-1 and Alexa Fluor 633) was determined (Fig. 6). Donor quenching arises due to sensitized emission, but also depends on competition effects. The latter can be neglected because of a minimal bleed-through in excitation of the used FRET pair YOYO-1 and Alexa Fluor 633. The donor quenching increased with increasing NP ratio indicating an enhanced stability of polyplexes with increasing NP ratio. The enhanced stability of polyplexes may be due to more LPEI available for polyplex formation. The FRET efficiency E on a cell-by-cell basis could not be calculated because the donor and acceptor concentration was not saturated and their conjungate-to-dye ratio r unknown. However, as it is most likely that the proportion of polymer to DNA is not constant in different polyplexes of single cells, acceptor sensitized emission as average

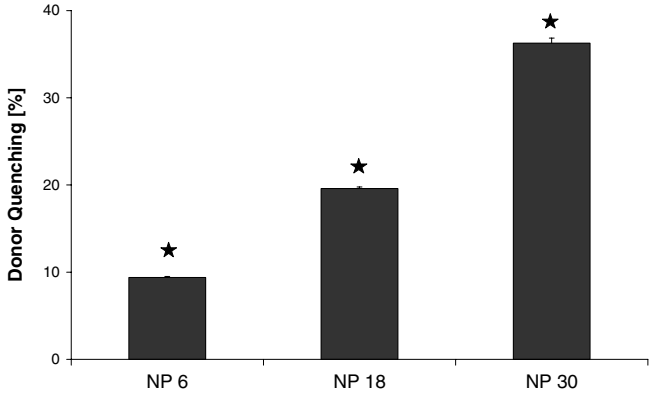

Fig. 6. Donor quenching of double labeled LPEI 5.0-polyplexes at NP 6, 18, and 30 after 6 h of transfection as determined by flow cytometry. Statistically significant differences between NP ratios are denoted by ★ ($\alpha < 0.01$).

value for the whole cell population meets the situation better than a cell-by-cell evaluation.

5. Conclusions

In this study, FRET was evaluated as tool to determine the intracellular disintegration of double labeled LPEI-polyplexes in CHO-K1 cells. In microscopy, two approaches have been considered for quantitative FRET analysis: sensitized emission measurement and acceptor photobleaching. Applying the acceptor photobleach method, the results were not accurate because of movements of or in the sample during the imaging process. Therefore, we would not recommend acceptor photobleaching for this application. Sensitized emission measurement using the method according to Xia and Liu [18] worked quite well for the determination of interaction between LPEI and plasmid DNA. Generally, we would advise caution for the investigation of interaction of polymer and plasmid DNA in living samples by FRET because of movement during the imaging process, but working with fixed cells is not an alternative because fixation agents may alter the structure of polyplexes. Furthermore, FRET occurring between two fluorescent molecules in LPEI-polyplexes was also successfully measured by flow cytometry. The advantage of the flow cytometry-based method is the analysis of a whole cell population.

With the established methods it is now possible to evaluate the intracellular stability of polyplexes built with various polymers at different NP ratios. We suggest that FRET is a useful tool in order to gain a deeper insight into LPEI-mediated gene transfer.

Acknowledgements

The authors thank Allison Dennis from the Georgia Institute of Technology for the careful revision of this manuscript. Furthermore, we thank Ralph Graef from Carl Zeiss Jena GmbH for his assistance with the sensitized emission measurements at the confocal microscope.

References

[1] J.-P. Behr, Gene transfer with synthetic cationic amphiphiles: prospects for gene therapy, Bioconjug. Chem. 5 (1994) 382–389.
[2] T. Bieber, W. Meissner, S. Kostin, A. Niemann, H.P. Elsasser, Intracellular route and transcriptional competence of polyethylenimine–DNA complexes, J. Control. Release 82 (2002) 441–454.
[3] M. Ogris, P. Steinlein, M. Kursa, K. Mechtler, R. Kircheis, E. Wagner, The size of DNA/transferrin-PEI complexes is an important factor for gene expression in cultured cells, Gene Ther. 5 (1998) 1425–1433.
[4] R. Wattiaux, N. Laurent, S. Wattiaux-De Coninck, M. Jadot, Endosomes, lysosomes: their implication in gene transfer, Adv. Drug Deliv. Rev. 41 (2000) 201–208.
[5] C. Goncalves, E. Mennesson, R. Fuchs, J.P. Gorvel, P. Midoux, C. Pichon, Macropinocytosis of polyplexes and recycling of plasmid via the clathrin-dependent pathway impair the transfection efficiency of human hepatocarcinoma cells, Mol. Ther. 10 (2004) 373–385.
[6] M. Breunig, U. Lungwitz, R. Liebl, C. Fontanari, J. Klar, A. Kurtz, T. Blunk, A. Goepferich, Gene delivery with low molecular weight linear polyethylenimines, J. Gene Med. 7 (2005) 1287–1298.
[7] K. Itaka, A. Harada, Y. Yamasaki, K. Nakamura, H. Kawaguchi, K. Kataoka, In situ single cell observation by fluorescence resonance energy transfer reveals fast intra-cytoplasmic delivery and easy release of plasmid DNA complexed with linear polyethylenimine, J. Gene Med. 6 (2004) 76–84.
[8] H.J. Kong, J. Liu, K. Riddle, T. Matsumoto, K. Leach, D.J. Mooney, Non-viral gene delivery regulated by stiffness of cell adhesion substrates, Nat. Mater. 4 (2005) 460–464.
[9] T. Foerster, Energy migration and fluorescence, Naturwissenschaften 33 (1946) 166–175.
[10] T. Foerster, Intermolecular energy transference and fluorescence, Ann. Phys. [6 Folge] 2 (1948) 55–75.
[11] E.A. Jares-Erijman, T.M. Jovin, FRET imaging, Nat. Biotechnol. 21 (2003) 1387–1395.
[12] P.G. Wu, L. Brand, Resonance energy transfer: methods and applications, Anal. Biochem. 218 (1994) 1–13.
[13] L. Stryer, Fluorescence energy transfer as a spectroscopic ruler, Annu. Rev. Biochem. 47 (1978) 819–846.
[14] J. Szollosi, P. Nagy, Z. Sebestyen, S. Damjanovich, J.W. Park, L. Matyus, Applications of fluorescence resonance energy transfer for mapping biological membranes, Rev. Mol. Biotechnol. 82 (2002) 251–266.
[15] J. Szollosi, S. Damjanovich, L. Matyus, Application of fluorescence resonance energy transfer in the clinical laboratory: routine and research, Cytometry 34 (1998) 159–179.
[16] C. Berney, G. Danuser, FRET or no FRET: a quantitative comparison, Biophys. J. 84 (2003) 3992–4010.
[17] G.W. Gordon, G. Berry, X.H. Liang, B. Levine, B. Herman, Quantitative fluorescence resonance energy transfer measurements using fluorescence microscopy, Biophys. J. 74 (1998) 2702–2713.
[18] Z. Xia, Y. Liu, Reliable and global measurement of fluorescence resonance energy transfer using fluorescence microscopes, Biophys. J. 81 (2001) 2395–2402.
[19] D.C. Youvan, C.M. Silva, E.J. Bylina, W.J. Coleman, M.R. Dilworth, M.M. Yang, Calibration of fluorescence resonance energy transfer in microscopy using genetically engineered GFP derivatives on nickel chelating beads, Biotechnology 3 (1997) 1–18.
[20] TASC Carl-Zeiss Jena, Geschaeftsbereich AIM, 2005.
[21] P.I. Bastiaens, T.M. Jovin, Microspectroscopic imaging tracks the intracellular processing of a signal transduction protein: fluorescent-labeled protein kinase C beta I, Proc. Natl. Acad. Sci. USA 93 (1996) 8407–8412.
[22] F.S. Wouters, P.I.H. Bastiaens, K.W.A. Wirtz, T.M. Jovin, FRET microscopy demonstrates molecular association of non-specific lipid transfer protein (nsL-TP) with fatty acid oxidation enzymes in peroxisomes, EMBO J. 17 (1998) 7179–7189.
[23] A.K. Kenworthy, Imaging protein-protein interactions using fluorescence resonance energy transfer microscopy, Methods 24 (2001) 289–296.
[24] T.S. Karpova, C.T. Baumann, L. He, X. Wu, A. Grammer, P. Lipsky, G.L. Hager, J.G. McNally, Fluorescence resonance energy transfer from cyan to yellow fluorescent protein detected by acceptor photobleaching using confocal microscopy and a single laser, J. Microsc. 209 (2003) 56–70.
[25] H. Amiri, G. Schultz, M. Schaefer, FRET-based analysis of TRPC subunit stoichiometry, Cell Calcium 33 (2003) 463–470.
[26] P. Batard, J. Szollosi, I. Luescher, J.C. Cerottini, R. MacDonald, P. Romero, Use of phycoerythrin and allophycocyanin for fluorescence resonance energy transfer analyzed by flow cytometry: advantages and limitations, Cytometry 48 (2002) 97–105.
[27] Z. Sebestyen, P. Nagy, G. Horvath, G. Vamosi, R. Debets, J.W. Gratama, D.R. Alexander, J. Szollosi, Long wavelength fluorophores and cell-by-cell correction for autofluorescence significantly improves the accuracy of flow cytometric energy transfer measurements on a dual-laser bench top flow cytometer, Cytometry 48 (2002) 124–135.

[28] A. Pfeiffer, A. Bottcher, E. Orso, M. Kapinsky, P. Nagy, A. Bodnar, I. Spreitzer, G. Liebisch, W. Drobnik, K. Gempel, M. Horn, S. Holmer, T. Hartung, G. Multhoff, G. Schutz, H. Schindler, A.J. Ulmer, H. Heine, F. Stelter, C. Schutt, G. Rothe, J. Szollosi, S. Damjanovich, G. Schmitz, Lipopolysaccharide and ceramide docking to CD14 provokes ligand-specific receptor clustering in rafts, Eur. J. Immunol. 31 (2001) 3153–3164.

[29] J. Szollosi, S. Damjanovich, S.A. Mulhern, L. Tron, Fluorescence energy transfer and membrane potential measurements monitor dynamic properties of cell membranes: a critical review, Prog. Biophys. Mol. Biol. 49 (1987) 65–87.

[30] J. Szollosi, L. Tron, S. Damjanovich, S.H. Helliwell, D. Arndt-Jovin, T.M. Jovin, Fluorescence energy transfer measurements on cell surfaces: a critical comparison of steady-state fluorimetric and flow cytometric methods, Cytometry 5 (1984) 210–216.

[31] L. Tron, J. Szollosi, S. Damjanovich, S.H. Helliwell, D.J. Arndt-Jovin, T.M. Jovin, Flow cytometric measurement of fluorescence resonance energy transfer on cell surfaces. Quantitative evaluation of the transfer efficiency on a cell-by-cell basis, Biophys. J. 45 (1984) 939–946.

[32] H.S. Rye, S. Yue, D.E. Wemmer, M.A. Quesada, R.P. Haugland, R.A. Mathies, A.N. Glazer, Stable fluorescent complexes of double-stranded DNA with bis-intercalating asymmetric cyanine dyes: properties and applications, Nucleic Acids Res. 20 (1992) 2803–2812.

[33] M. Wong, S. Kong, W.H. Dragowska, M.B. Bally, Oxazole yellow homodimer YOYO-1-labeled DNA: a fluorescent complex that can be used to assess structural changes in DNA following formation and cellular delivery of cationic lipid DNA complexes, Biochim. Biophys. Acta 1527 (2001) 61–72.

[34] G. Krishnamoorthy, G. Duportail, Y. Mely, Structure and dynamics of condensed DNA probed by 1,1′-(4,4,8,8-Tetramethyl-4,8-diazaundecamethylene)bis[4-[[3- methylbenz-1,3-oxazol-2-yl]methylidine]-1,4-dihydroquinolinium] tetraiodide fluorescence, Biochemistry 41 (2002) 15277–15287.

[35] C. Madeira, L.M.S. Loura, M.R. Aires-Barros, A. Fedorov, M. Prieto, Characterization of DNA/lipid complexes by fluorescence resonance energy transfer, Biophys. J. 85 (2003) 3106–3119.

[36] D. Lleres, E. Dauty, J.P. Behr, Y. Mely, G. Duportail, DNA condensation by an oxidizable cationic detergent. Interactions with lipid vesicles, Chem. Phys. Lipids 111 (2001) 59–71.

[37] U. Lungwitz, M. Breunig, T. Blunk, A. Goepferich, Synthesis and application of low molecular weight linear polyethylenimines for non-viral gene deliver, in: Proceedings of the Annual Meeting of the German Pharmaceutical Society, 2004, PT25, 157.